

Flexible Bonding of the Phosph(V)azane Dianions  $[\text{S}(\text{E})\text{P}(\mu\text{-N}^t\text{Bu})_2]^{2-}$ Alex J. Plajer,<sup>[a]</sup> Raul Garcia-Rodriguez,<sup>[b]\*</sup> Felix J. Rizzuto<sup>[a]</sup> and Dominic S. Wright.<sup>[a]\*</sup>

**Abstract:** Oxidation of the P(III) dianion  $[\text{S-P}(\mu\text{-N}^t\text{Bu})_2]^{2-}$  (**1**) with elemental sulphur, selenium and tellurium gives the P(V) dianions  $[\text{S}(\text{E})\text{P}(\mu\text{-N}^t\text{Bu})_2]^{2-}$  (E = S (**6a**), Se (**6b**), Te (**6c**)). Although **6c** proves to be too unstable, the S,S-dianion **6a** and ambidentate S,Se-dianion **6b** are readily transferred *intact* to main group and transition metal elements, producing a range of new cage and coordination compounds. While their coordination characteristics are in many ways similar to closely-related isoelectronic phosph(V)azane anions  $[(\text{E})(\text{RN}=\text{P}(\mu\text{-N}^t\text{Bu}))_2]^{2-}$ , the sterically unhindered nature of **6** introduces an expanded range of coordination modes, i.e., facial S,S- and Se,Se-bonding as well as side-on S,Se-coordination. All of these bonding modes are observed for the ambidentate S,Se dianion **6b**.

## Introduction

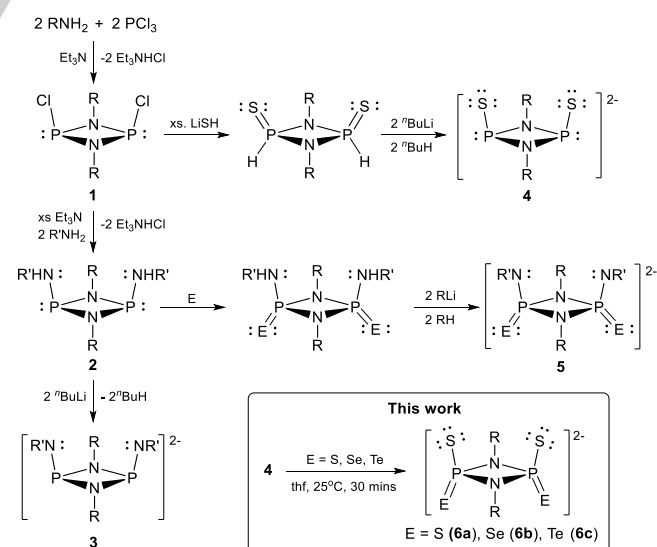
Inorganic ligands (based on non-carbon frameworks) have great potential in coordination chemistry and as readily-modified ligands for single-site organometallic catalysis.<sup>[1,2]</sup> There are several general advantages of inorganic arrangements over traditional carbon-based ligand systems. In particular, the greater number of elements available and broader range of geometries across the entire spectrum of the periodic table provides the potential for greater tuning of steric and electronic properties within a given class of ligands. Owing to the relatively high bond energy of single P–N bonds (290 kJ mol<sup>-1</sup>) compared to C–C bonds (350 kJ mol<sup>-1</sup>), phosph(III/V)azanes are excellent candidates for the construction of a range of new ligand systems.

A major focus of research over the past 20 years has been on macrocyclic and acyclic ligands derived from the simple cyclodiphosph(III)azane building blocks  $[\text{CIP}(\mu\text{-NR})_2]$  (**1**).<sup>[3]</sup> A particularly well-studied class of phosph(III)azane ligands, which illustrate the ease by which such ligands can be obtained, are the P,P-dithio-1,3,2,4-diazadiphosphetidine dianions  $[(\text{R}'\text{N})\text{P}(\mu\text{-NR})_2]^{2-}$  (**3**), obtained from the

deprotonation of  $[(\text{R}'\text{NH})\text{P}(\mu\text{-NR})_2]$  (**2**) (Scheme 1).<sup>[3a]</sup> Ligands **3** have been shown to have extensive coordination chemistry with a broad range of main group elements and transition metals. Simple modulation strategies allow extensive variation of the ligand set (R and R').

We recently reported the syntheses and structures of the Na<sup>+</sup> and Mg<sup>2+</sup> salts of the P(III) dianion  $[(\text{S})\text{P}(\mu\text{-N}^t\text{Bu})_2]^{2-}$  (**4**), which is valence-isoelectronic with **3** (Scheme 1).<sup>[4]</sup> We also showed that the reduced steric demands of this ligand and the presence of hard/soft (N/S) donor atoms make **4** of particular interest in metal cage formation and in adaptable coordination to a range of metal centers. However, one problem encountered during these studies is that Lewis acidic metals in particular result in dimerisation of **4** *via* the elimination of metallsulphides to give  $[\text{S}(\text{H})\text{P}(\mu\text{-N}^t\text{Bu})_2\text{P}(\mu\text{-S})\text{P}(\mu\text{-N}^t\text{Bu})_2\text{P}(\text{H})=\text{S}]$ . To date, this instability has restricted more extensive studies in this area.

Relevant to the current study, Chivers and Woolins have explored related P(V) dianionic ligands. The oxidative addition of chalcogens (E = S, Se) to **2** gives the neutral P(V) species  $[\text{tBuNH}(\text{E}=\text{P}(\mu\text{-N}^t\text{Bu}))_2]$ , which are readily deprotonated to give the dianions  $[\text{tBuN}(\text{E})\text{P}(\mu\text{-N}^t\text{Bu})_2]^{2-}$  (**5**) (Scheme 1).<sup>[5b]</sup> The Te analogue, however, can only be obtained *via* oxidation of the dianion  $[(\text{tBuN})\text{P}(\mu\text{-N}^t\text{Bu})_2]^{2-}$  with Te.<sup>[5a]</sup> These ligands mainly exhibit E,E-facial bonding to a range of transition and main group elements, although side-on (tBuN)N,E-bonding has also been observed in a few cases.<sup>[6]</sup>



Scheme 1: Stepwise build-up of cyclodiphosphazane ligands.

[a] Prof. D. S. Wright, Mr. A. Plajer, Mr. Felix J. Rizzuto  
Chemistry Department  
Cambridge University  
Lensfield Road, Cambridge CB2 1EW (U.K.)  
E-mail: [dsw1000@cam.ac.uk](mailto:dsw1000@cam.ac.uk)

[b] Dr. R. Garcia-Rodriguez, GIR MIOMeT-IU Cinquma-Química  
Inorgánica, Facultad de Ciencias, Campus Miguel, Delibes,  
Universidad de Valladolid 47011 Valladolid, Spain.

## FULL PAPER

Here we report that the oxidative addition of S, Se and Te to the sodium salt of the P(III) dianion **4** under mild conditions yields the dianions  $[S(E)P(\mu\text{-N}^t\text{Bu})_2]^{2-}$  [ $E = \text{S}$  (**6a**), Se (**6b**), Te (**6c**)], which are valence-isoelectronic with **5**. Studies of the coordination chemistry of **6a** and **6b** with main group and transition metal elements show that these anions can be transferred *intact*, having similar features to previously explored P(V) dianions **5**, but with reduced steric demands and an increased number of coordination modes. An interesting feature in this regard is the competition exhibited between the various bonding modes to metal and non-metal centers.

## Results and Discussion

Our primary motivation for the investigation of the oxidation of the P(III) dianion **4** with chalcogens was to improve its thermodynamic stability, overcoming the difficulties observed in attempts to coordinate it to Lewis acidic metals, and its air-stability, making it more amenable as a ligand in general.

Using a similar synthetic procedure to that reported by Chivers for the Te analogue of **5**,  $[\text{RN}=(\text{Te})\text{P}(\mu\text{-NR})_2]^{2-}$ ,<sup>[5a]</sup> the sodium salts of **6a**, **6b** and **6c** were prepared by room-temperature reactions of the dianion **4** [generated *in situ* by deprotonation of  $[\text{S}=(\text{H})\text{P}(\mu\text{-}^t\text{Bu})_2]$  with  $\text{BnNa}$  ( $\text{Bn} = \text{benzyl}$ )] with two equivalents of solid S, Se or Te in thf. The products  $\text{Na}_2[\text{S}(\text{E})\text{P}(\mu\text{-N}^t\text{Bu})_2] \cdot 0.5\text{thf}$  [ $E = \text{S}$  ( $\text{Na}_2\mathbf{6a} \cdot 0.5\text{thf}$ ), Se ( $\text{Na}_2\mathbf{6b} \cdot 0.5\text{thf}$ ) and Te ( $\text{Na}_2\mathbf{6c} \cdot 0.5\text{thf}$ )] were isolated as powders in high yields (91–95%) after removal of the solvent and precipitation with toluene. The salts were fully characterised using a combination of elemental analysis and multinuclear ( $^1\text{H}$ ,  $^{31}\text{P}$ ,  $^{77}\text{Se}$ ,  $^{125}\text{Te}$ ) NMR spectroscopy (Supporting Information). An important point to note is that, as in the case of the previously reported dianions **5**, oxidative addition of S, Se and Te appears to occur only at one  $\text{P}_2\text{N}_2$  face of **4**, giving exclusive formation of the *cis*-isomers of the dianions **6b** and **6c** (as depicted in Scheme 1). An alternative route to **6a-c** through oxidation of the neutral precursor  $[\text{S}=(\text{H})\text{P}(\mu\text{-N}^t\text{Bu})_2]$  with S or Se, analogous to that used to access the previously reported for the S and Se homologues of the anions **5**,<sup>[5b]</sup> resulted in decomposition.

In the case of the reaction with S, formation of the anion **6a** is indicated by the large change in chemical shift observed in the  $^{31}\text{P}\{^1\text{H}\}$  NMR spectrum at room temperature in thf, from a broad singlet at  $\delta = 190$  ppm for **4** to a very sharp singlet at  $\delta = 87$  ppm which is symptomatic of the change in oxidation state of the cyclophosphazane phosphorus atoms from P(III) to P(V). Oxidation of the sodium salt of **4** with selenium is also accompanied by a similar change in chemical shift, with the anion **6b** exhibiting a sharp singlet at  $\delta = 57.5$  ppm in the  $^{31}\text{P}\{^1\text{H}\}$  NMR spectrum, together with  $^{77}\text{Se}$  satellites ( $^1J_{\text{P-Se}} = 703$ ,  $^2J_{\text{P-P}} = 10.1$  Hz). The latter are the result of the presence of a minor isotopomer of the **6b** (i.e.,  $[\text{S}-(^{77}\text{Se})\text{P}(\mu\text{-N}^t\text{Bu})_2\text{P}(\text{=Se})\text{-S}]^{2-}$ ). The  $^1J_{\text{P-Se}}$  coupling can also be observed in the  $^{77}\text{Se}$  NMR spectrum of **6b**, giving a doublet at  $\delta = 259.9$  ppm with  $^1J_{\text{P-Se}} = 695.5$  Hz.

Both  $[\text{Na}_2\mathbf{6a} \cdot 0.5\text{thf}]$  and  $[\text{Na}_2\mathbf{6b} \cdot 0.5\text{thf}]$  crystallize as complicated, highly disordered coordination networks which make crystallographic analysis and meaningful discussion of structural parameters difficult. As a result, their structures are

not reported here. However, metathesis of the sodium salt of **6a** with  $^t\text{BuNH}_3\text{Cl}$  yields the ammonium salt  $[(^t\text{BuNH}_3)_2(\text{thf})_2\mathbf{6a}]$  which crystallizes as discrete molecular units (Fig. 1) (Supporting Information). In the solid-state structure two  $^t\text{BuNH}_3^+$  cations symmetrically bridge the phosphazane dianion at its top and bottom faces *via* N-H...S H-bonds (with the remaining N-H-atom of each of the  $^t\text{BuNH}_3^+$  cations being H-bonded to thf O-atoms). The observed P-S bond lengths are relatively uniform within the dianion unit **6a** (1.9917(5)–1.9939(5) Å) and are probably best described as part-way between P-S (ca. 2.2–2.3 Å) single and P=S double bonds (ca. 1.9–2.0 Å).<sup>[7]</sup> This situation can be compared to those in which **6a** is bonded to a range of main group and transition metal atoms (described later in this paper), where redistribution towards distinct P-S and P=S bonding is found within the framework of **6a**.

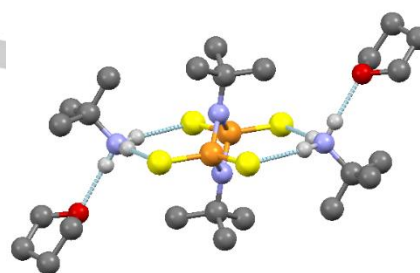
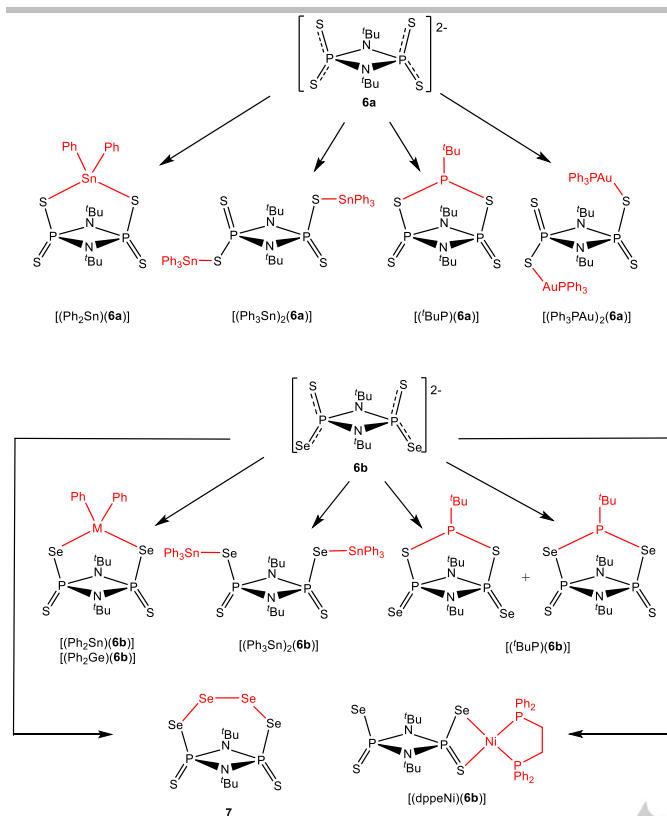


**Fig. 1:** Solid-state structure of  $[(^t\text{BuNH}_3)_2(\text{thf})_2\mathbf{6a}]$ . Selected bond lengths (Å) and angles ( $^\circ$ ): P-N 1.7022(5)–1.7023(5), P-S 1.9917(5)–1.9939(5), N...S 3.256(5)–3.274(5) [N-H...S 2.30(2)–2.31(2)], P-N-P 96.92(6), N-P-N 83.08(6), S-P-S 111.51(2). Colour code, S (yellow), P (orange), N (violet), O (red).

Room-temperature oxidation of **4** with elemental Te yields the telluride anion  $[\text{S}(\text{Te})\text{P}(\mu\text{-N}^t\text{Bu})_2]^{2-}$  (**6c**), indicated by appearance of a singlet at  $\delta = -32.2$  ppm accompanied by  $^{125}\text{Te}$  satellites in the  $^{31}\text{P}$  NMR spectrum at room temperature (Supporting Information). Again formation of the asymmetric isotopomer  $[\text{S}(^{125}\text{Te})\text{P}(\mu\text{-N}^t\text{Bu})_2\text{P}(\text{Te})\text{S}]^{2-}$  causes splitting of the  $^{125}\text{Te}$  satellites ( $^1J_{\text{P-Te}} = 1638$  Hz) into doublets ( $^2J_{\text{P-P}}$  coupling of 18.8 Hz). Strongly-shielded P(V) centers in cyclophosphazane ditellurides were also observed by Woollins *et al.* for the  $[\text{tBuN}=(\text{Te})\text{P}(\mu\text{-N}^t\text{Bu})_2]^{2-}$  dianion, which has a resonance at  $\delta = -74.9$  ppm in the  $^{31}\text{P}$  NMR spectrum.<sup>[6d]</sup> The  $^{125}\text{Te}$  NMR spectrum of **6c** shows the expected doublet at  $\delta = 420.1$  ppm ( $^1J_{\text{P-Te}} = 1638$  Hz). Unlike the salts of **6a** and **6b**, the solid sodium salt  $[\text{Na}_2\mathbf{6c} \cdot 0.5\text{thf}]$  is extremely unstable and decomposes to give Te metal even at low temperature and in the absence of light in a few days. This is not unexpected for P-Te bonded species, which have been shown to decompose rapidly due to the lability of the P-Te bond.

In contrast to the Te dianion **6c**, the S- and Se- anions **6a** and **6b** are storable over the course of months under an  $\text{N}_2$  atmosphere at room temperature. As a consequence, further investigations of the coordination chemistry of these ligands focused on these species. The products formed by reactions of the sodium salts of **6a** and **6b** ( $[\text{Na}_2\mathbf{6a} \cdot 0.5\text{thf}]$ , Se ( $\text{Na}_2\mathbf{6b} \cdot 0.5\text{thf}$ )] with a range of main group and transition element precursors undertaken in the current study are summarised in Scheme 2 (which also gives the numbering scheme used in the following discussion).



**Scheme 2** Reactions undertaken and products formed in the current study.

The 1 : 1 stoichiometric reactions of the sodium salts  $[\text{Na}(\text{thf})_{0.5}\mathbf{6a}]$  and  $[\text{Na}_2(\text{thf})_{0.5}\mathbf{6b}]$  with  $\text{Ph}_2\text{SnCl}_2$  and  $\text{Ph}_2\text{GeCl}_2$  in thf produce similar cages, which result from metal-exchange of the  $\text{Na}^+$  cations for Sn(IV) and Ge(IV). The new cages  $[\text{Ph}_2\text{Sn}(\mathbf{6a})]$ ,  $[\text{Ph}_2\text{Sn}(\mathbf{6b})]$  and  $[\text{Ph}_2\text{Ge}(\mathbf{6b})]$  were obtained as crystals in moderate yields of 60–66% after work up and were fully characterised (Scheme 2 and Supporting Information). The stabilisation effect of S- or Se-oxidation on the framework of the P(III) dianion  $[(\text{S})\text{P}(\mu\text{-N}'\text{Bu})_2]^{2-}$  (**4**) is indicated in particular by the fact that whereas the P(V) compound  $[\text{Ph}_2\text{Sn}(\mathbf{6b})]$  exhibits some limited stability in air and prolonged thermal stability under inert atmosphere in the solid state and in solution, the previously reported un-oxidised P(III) analogue  $[\text{Ph}_2\text{Sn}(\mathbf{4})]$  is very air sensitive and highly unstable (decomposing into Sn metal even under inert atmosphere in solution).<sup>[4b]</sup>

The formation of the Sn(IV) complex  $[\text{Ph}_2\text{Sn}(\mathbf{6a})]$  is confirmed in the room-temperature  $^{119}\text{Sn}$  NMR spectrum of the isolated product in  $\text{C}_6\text{D}_6$ , which shows a triplet at  $\delta = -134.1$  ppm as a result of coupling to the two magnetically-equivalent P-atoms of **6a** ( $\delta = 134.1$  Hz,  $^2J_{\text{P-Sn}} = 49$  Hz). Crystals of  $[\text{Ph}_2\text{Sn}(\mathbf{6a})]$  suitable for X-ray analysis were grown from a saturated solution of *n*-hexane at room temperature. The solid-state structure of  $[\text{Ph}_2\text{Sn}(\mathbf{6a})]$  has a bicyclic arrangement in which the  $[(\text{S})\text{S}(\text{P}(\mu\text{-N}'\text{Bu}))_2]^{2-}$  dianion **6a** chelates the  $\text{Ph}_2\text{Sn}$  unit (Fig. 2a). The four S atoms of the dianion lie in a plane, perpendicular to the almost planar  $\text{P}_2\text{N}_2$  ring unit. The steric congestion between the  $t\text{Bu}$  groups within the  $\text{P}_2\text{N}_2$  ring of the dianion and the Ph-groups of the  $\text{SnPh}_2$  unit results in noticeable distortions within the structure, in

which the  $\text{SnPh}_2$  group tilts towards one side of the  $\text{P}_2\text{N}_2$  ring unit. Coordination of the Sn(IV) center results in a decrease in the  $\text{S}\cdots\text{S}$  contact distance at the metal-coordination side of the dianion relative to the uncoordinated side of ca. 0.45 Å. A further difference between the dianion of  $[(t\text{BuNH}_3)_2(\text{thf})_2\mathbf{6a}]$  and the dianion unit of  $[\text{Ph}_2\text{Sn}(\mathbf{6a})]$  is the redistribution towards distinct P-S(Sn) (mean 2.08 Å) and P=S (mean 1.92 Å) bonding (cf. the intermediate bonding observed in bonding in  $[(t\text{BuNH}_3)_2(\text{thf})_2\mathbf{6a}]$ ).

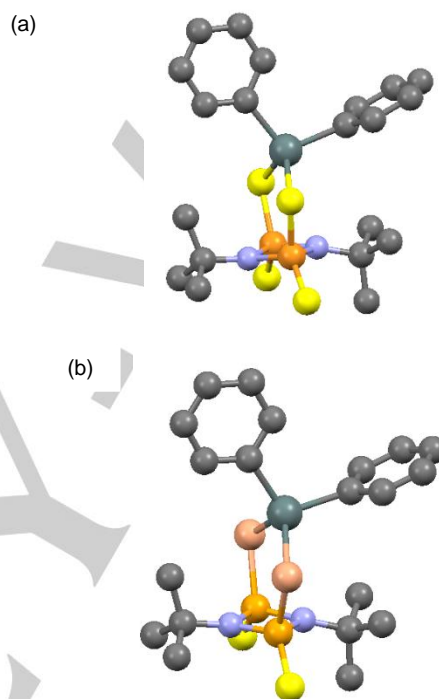


**Fig. 2** Molecular structures of the cages (a)  $[\text{Ph}_2\text{Sn}(\mathbf{6a})]$  and (b)  $[\text{Ph}_2\text{Sn}(\mathbf{6b})]$ . Only one of the two independent molecules in the unit cells of both compounds is shown. H-atoms have been omitted for clarity. Selected bond lengths (Å) and angles ( $^\circ$ ): Molecular structure of the cage  $[\text{Ph}_2\text{Sn}(\mathbf{6b})]$ . H-atoms have been omitted for clarity. Selected bond lengths (Å) and angles ( $^\circ$ ):  $[\text{Ph}_2\text{Sn}(\mathbf{6a})]$ , Sn-S mean range 2.4375(11)–2.4468(11), P-S(Sn) range 2.0750(15)–2.0873(14), P=S mean range 1.9132(15)–1.9172(15), P-N range 1.680(4)–1.693(3), S-Sn-S range 111.04(4)–111.61(4), P-S-Sn range 100.36(5)–101.00(5), P-N-P range 94.94(17)–95.68(17), N-P-N range 83.98(17)–84.67(17), S-P-S mean 109.35(7)–110.62(7), the  $\text{Ph}_2\text{Sn}$  unit is puckered by a mean of  $20.5^\circ$  out of the  $\text{P}\cdots\text{PS}_2\text{Sn}$  ring unit.  $[\text{Ph}_2\text{Sn}(\mathbf{6b})]$ , Sn-Se mean 2.5605(7)–2.5571(6), P-Se mean 2.2226(14)–2.2398(14), P=S mean 1.9172(19)–1.9191(17), P-N mean 1.679(4)–1.702(4), Se-Sn-Se mean 112.34(2)–112.90(2), P-Se-Sn mean 98.37(4)–98.98(4), P-N-P mean 95.2(2)–95.8(2), N-P-N mean 83.9(2)–84.8(2), Se-P-S mean 108.37(8)–109.91(7), the  $\text{Ph}_2\text{Sn}$  unit is puckered by a mean of  $19.7^\circ$  out of the  $\text{P}\cdots\text{PSe}_2\text{Sn}$  ring unit. Colour code, S (yellow), P (orange), N (violet), Se (pink), Sn (green).

The room-temperature  $^{31}\text{P}$  NMR spectrum of  $[\text{Ph}_2\text{Sn}(\mathbf{6b})]$  in  $\text{C}_6\text{D}_6$  is more complicated than for the complex with **6a**, owing to the presence of NMR-active  $^{77}\text{Se}$ . The result is that the singlet observed in the room-temperature  $^{31}\text{P}$  NMR spectrum of  $[\text{Ph}_2\text{Sn}(\mathbf{6b})]$  ( $\delta = 34.9$  ppm) is flanked by  $^{77}\text{Se}$  and  $^{117/119}\text{Sn}$  satellites ( $t, ^1J_{\text{P-Se}} = 463$  Hz,  $^2J_{\text{P-Sn}} = 69$  Hz). Like  $[\text{Ph}_2\text{Sn}(\mathbf{6a})]$ , the  $^{119}\text{Sn}$  NMR spectrum shows a triplet resonance at  $\delta = -54.2$  ppm ( $^2J_{\text{P-Sn}} = 69$  Hz), resulting from the coupling of the Sn(IV) bridge to the two equivalent P-atoms in the  $\text{P}_2\text{N}_2$  ring. However, neither the  $^{31}\text{P}$  NMR nor the  $^{119}\text{Sn}$  NMR spectra give any insight into whether the Sn(IV) atom is S,S- or Se,Se-chelated, since the NMR data for both modes

## FULL PAPER

should be similar.<sup>[6d]</sup> This uncertainty is resolved by the solid-state structure of  $[\text{Ph}_2\text{Sn}(\mathbf{6b})]$ , crystals of which were obtained from a saturated solution of the complex in *n*-hexane at room temperature. Single-crystal X-ray analysis shows that the ligand **6b** adopts the Se,Se-coordination mode in  $[\text{Ph}_2\text{Sn}(\mathbf{6b})]$  (Fig. 2b). The same type of steric confrontation between the <sup>t</sup>Bu groups of the  $\text{P}_2\text{N}_2$  ring and the  $\text{Ph}_2\text{Sn}$  unit is found in  $[\text{Ph}_2\text{Sn}(\mathbf{6b})]$  as was seen previously in the structure of  $[\text{Ph}_2\text{Sn}(\mathbf{6a})]$ , resulting in the tilting of the  $\text{Ph}_2\text{Sn}$  unit towards one side of the molecule. The room-temperature NMR spectroscopic behaviour and solid-state structural arrangement of the Ge(IV) cage  $[\text{Ph}_2\text{Ge}(\mathbf{6b})]$  are similar to that of the Sn(IV) analogue, again showing Se,Se-facial bonding to the Ge(IV) center (see Supporting Information). The structural arrangement found for  $[\text{Ph}_2\text{Sn}(\mathbf{6a})]$ ,  $[\text{Ph}_2\text{Sn}(\mathbf{6b})]$  and  $[\text{Ph}_2\text{Ge}(\mathbf{6b})]$  is similar to that seen previously for  $\text{R}_2\text{Ge}^-$  and  $\text{R}_2\text{Sn}^-$  complexes of the dianions **5**.<sup>[6d]</sup>

The reactions of the sodium salts of **6a** and **6b** with 2 equivalents of  $\text{Ph}_3\text{SnCl}$  give the Sn(IV) compounds  $[(\text{Ph}_3\text{Sn})_2(\mathbf{6a})]$  and  $[(\text{Ph}_3\text{Sn})_2(\mathbf{5b})]$  in 80% and 56% yields, respectively (see Supporting Information). The formation of a Sn(IV) compound is easily seen in the  $^{119}\text{Sn}$  NMR spectrum of  $[(\text{Ph}_3\text{Sn})_2(\mathbf{6b})]$  which appears as a doublet due to coupling to the separate  $^{31}\text{P}$  atoms of the framework of **6b** ( $\delta = -113.2$  ppm,  $^2J_{\text{P-Sn}} 52$  Hz). In the case of  $[(\text{Ph}_3\text{Sn})_2(\mathbf{6a})]$ , however, only a broad singlet is seen in the  $^{119}\text{Sn}$  NMR spectrum ( $\delta = -107.5$  ppm). This variance provided an initial indication of a difference between the structural arrangement of  $[(\text{Ph}_3\text{Sn})_2(\mathbf{6b})]$  and  $[(\text{Ph}_3\text{Sn})_2(\mathbf{6a})]$ , which was later revealed in their solid-state structures.

Crystals of  $[(\text{Ph}_3\text{Sn})_2(\mathbf{6a})]$  were obtained from *n*-hexane, while crystals of  $[(\text{Ph}_3\text{Sn})_2(\mathbf{6b})]$  were grown from toluene [giving the solvate  $[(\text{Ph}_3\text{Sn})_2(\mathbf{6b})]\cdot 2\text{toluene}$ ]. The solid-state structures of both are shown Fig. 3. The (at first sight) surprising difference between them is the *trans*-S,S coordination observed in  $[(\text{Ph}_3\text{Sn})_2(\mathbf{6a})]$  (Fig. 3a) and the *cis*-Se,Se-coordination of the Sn(IV) centers in  $[(\text{Ph}_3\text{Sn})_2(\mathbf{6b})]$  (Fig. 3b). The *trans* structural arrangement of  $[(\text{Ph}_3\text{Sn})_2(\mathbf{6a})]$  is clearly the most stable alternative on steric grounds. However, owing to the *cis*-conformation of the S-atoms in the dianion **6b**, *trans* coordination of the Sn centers would have to occur using one Sn-S and one Sn-Se bond, leading to an unsymmetrical structure. A possible explanation for the observed *cis*-Se,Se isomer (as opposed to the *cis*-S,S alternative) is that the formation of two weaker Sn-Se bonds is compensated for by the retention of two stronger P=S bonds within the dianion framework, making the observed *cis*-Se,Se-isomer the most thermodynamically stable in this case. It is worthwhile noting that the dianion of  $[(\text{Ph}_3\text{Sn})_2(\mathbf{6a})]$  (like that of  $[\text{Ph}_2\text{Sn}(\mathbf{6a})]$ ) exhibits approximate P-S(Sn) single and P=S double bonding.

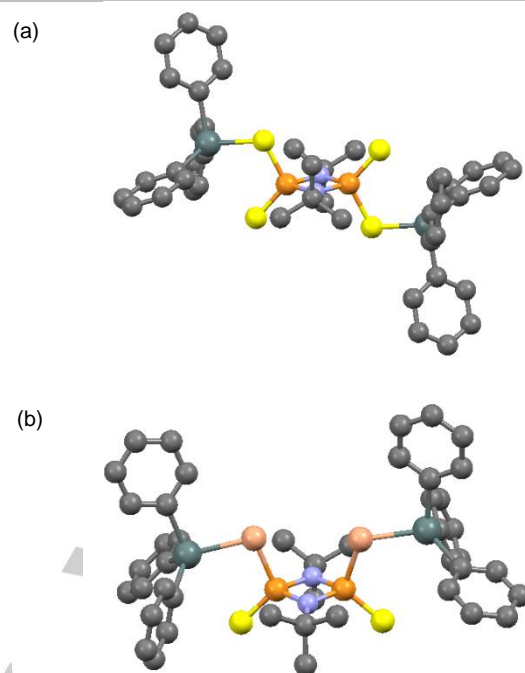
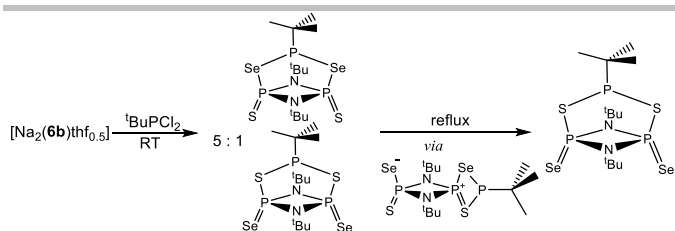


**Fig. 3** Molecular structures of (a)  $[(\text{Ph}_3\text{Sn})_2(\mathbf{6a})]$  and (b)  $[(\text{Ph}_3\text{Sn})_2(\mathbf{6b})]$ . Only one of the two independent molecules present in the unit cell of  $[(\text{Ph}_3\text{Sn})_2(\mathbf{6a})]$  is shown. H-atoms and lattice toluene molecules (in the case of the solvate  $[(\text{Ph}_3\text{Sn})_2(\mathbf{6b})]\cdot 2\text{toluene}$ ) have been omitted for clarity. Selected bond lengths (Å) and angles ( $^\circ$ ): Selected bond lengths (Å) and angles ( $^\circ$ ):  $[(\text{Ph}_3\text{Sn})_2(\mathbf{6a})]$ , Sn-S range 2.4479(8)-2.4522(8), P-S(Sn) range 2.0581(12)-2.0636(12), P=S range 1.9279(12)-1.9304(11), P-N range 1.680(3)-1.685(3), P-S-Sn range 104.51(4)-106.19(4), P-N-P range 96.41(14)-96.87(14), N-P-N range 83.12(15)-83.59(13), S-P=S range 112.86(5)-113.12(5).  $[(\text{Ph}_3\text{Sn})_2(\mathbf{6b})]$ , Sn-Se range 2.5552(5)-2.5556(5), P-Se range 2.2276(12)-2.2317(12), P=S range 1.9281(16)-1.9350(16), P-N range 1.688(3)-1.692(3), P-Se-Sn mean 100.36(3)-106.30(3), P-N-P range 95.79(16)-96.03(17), N-P-N range 83.96(16)-84.06(16), S-P=S range 114.83(6)-115.15(6). Colour code, S (yellow), P (orange), N (violet), Se (pink), Sn (green).

The reactions of **6a** and **6b** with non-metallic main group species were also explored. The reaction of  $[\text{Na}_2(\mathbf{6b})]\cdot 0.5\text{thf}$  with <sup>t</sup>BuPCl<sub>2</sub> at room temperature in thf gives  $[(\mathbf{6b})\text{P}^t\text{Bu}]$  as a mixture of two isomers in which the <sup>t</sup>BuP group is S,S- or Se,Se-bonded (in 1 : 5 ratio, respectively, Scheme 3) (see Supporting Information). The *in situ*  $^{31}\text{P}\{^1\text{H}\}$  NMR spectrum of the reaction mixture shows two triplets corresponding to the <sup>t</sup>BuP centers and two doublets for the  $\text{P}_2\text{N}_2$  ring atoms of each isomer. Interestingly, complete conversion of the Se,Se- into the S,S-isomer of  $[(\mathbf{6b})\text{P}^t\text{Bu}]$  occurs when the initial mixture of isomers is brought to reflux. Although reactions of the closely related dianions  $[\text{RN}=(\text{E})\text{P}(\mu\text{-NR})_2]^{2-}$  (E = S, Se, Te) (**5**) with a range of dichlorophosphines ( $\text{R}'\text{PCl}_2$ ) also form facially-bridged S,S- or Se,Se-cages of the type  $[(\mathbf{5})\text{PR}]$  (similar to  $[(\mathbf{6b})\text{P}^t\text{Bu}]$ ),<sup>[6c,d]</sup> zwitterionic side-on S,N-bonded isomers predominate for the S-dianion  $[\text{RN}=(\text{S})\text{P}(\mu\text{-NR})_2]^{2-}$ .<sup>[6d]</sup> However, a similar side-on Zwitterionic intermediate may be responsible for the conversion of the Se,Se-isomer to the S,S-isomer of  $[(\mathbf{6b})\text{P}^t\text{Bu}]$  (Scheme 3).



**Scheme 3** The two isomers of [(**6b**)P<sup>tBu</sup>] formed at room temperature and their conversion into the S,S-isomer, via a potential Zwitterionic intermediate.

The <sup>31</sup>P NMR spectrum of the pure S,S-isomer of [(**6b**)P<sup>tBu</sup>] in C<sub>6</sub>D<sub>6</sub> features a doublet at  $\delta = 37.4$  ppm and a triplet at  $\delta = 148.5$  ppm, both accompanied by a set of <sup>77</sup>Se satellites (<sup>1</sup>J<sub>P-P</sub> = 442, <sup>3</sup>J<sub>P-P</sub> = 206 Hz). As expected, these coupling constants are matched in the <sup>77</sup>Se NMR spectrum by a doublet of doublets signal at  $\delta = 303$  ppm. Interestingly, the <sup>1</sup>H NMR spectrum at room temperature shows two different chemical environments for the ring P<sub>2</sub>N<sub>2</sub> <sup>t</sup>Bu-substituents in 1:1 ratio at  $\delta = 1.71$  and 1.64 ppm. This is also seen in the <sup>1</sup>H NMR spectrum of the Se,Se-bridged isomer. The inequivalence of the ring <sup>t</sup>Bu groups results in both cases from the high energy barrier for lone-pair inversion at the phosphorus(III) center (Fig. 4). Variable-temperature <sup>1</sup>H NMR spectroscopic studies in toluene showed that there is no coalescence of the two <sup>t</sup>Bu-resonances for both isomers even at temperatures up to 80 °C.

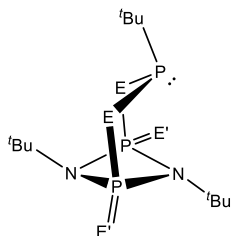


**Fig. 4** Structure of the Se,Se (E = Se, E' = S) and S,S- (E = S, E' = Se) isomers of [(**6b**)P<sup>tBu</sup>].

The above conclusions concerning the S,S- and Se,Se-isomers of [(**6b**)P<sup>tBu</sup>] are supported by the NMR spectroscopic behaviour and solid-state structure of the [(**6a**)P<sup>tBu</sup>], obtained from the 1 : 1 reaction of the [Na<sub>2</sub>(**6a**)0.5thf] with <sup>t</sup>BuPCL<sub>2</sub> in thf at room temperature (see Supporting Information). Owing to the extensive disorder present in [(**6a**)P<sup>tBu</sup>] it is not possible to discuss any of the bond lengths and angles in the single-crystal X-ray structure meaningfully. However, the molecular structure confirms the overall connectivity of the cage arrangement unambiguously, in which the disposition of the pyramidal P(III) atom of the <sup>t</sup>BuP group (with a stereochemically-active lone pair) results in the spatial inequivalence of the <sup>t</sup>Bu groups of the P<sub>2</sub>N<sub>2</sub> ring (Fig. 5). Like [(**6b**)P<sup>tBu</sup>], the room-temperature <sup>1</sup>H NMR spectrum of [(**6a**)P<sup>tBu</sup>] in C<sub>6</sub>D<sub>6</sub> shows three 1 : 1 : 1 <sup>t</sup>Bu resonances for the <sup>t</sup>Bu groups within the P<sub>2</sub>N<sub>2</sub> ring unit and in the <sup>t</sup>BuP group (at  $\delta = 1.71$  (s., <sup>t</sup>BuN), 1.64 (s., <sup>t</sup>BuN) and 1.00 ppm (d., <sup>t</sup>BuP, <sup>3</sup>J<sub>P-H</sub> = 12.3 Hz)). The <sup>31</sup>P{<sup>1</sup>H} NMR spectrum of [(**6a**)P<sup>tBu</sup>] at room-temperature in C<sub>6</sub>D<sub>6</sub> also shows a triplet resonance at  $\delta = 134.6$  ppm corresponding to the P(III) atom of the <sup>t</sup>BuP group and a doublet at  $\delta = 53.5$  ppm for the P<sub>2</sub>N<sub>2</sub> ring P(V) atoms. No such asymmetry is indicated in the room-temperature solution <sup>1</sup>H NMR spectra of [Ph<sub>2</sub>Sn(**6a**)] and

[Ph<sub>2</sub>Sn(**6b**)] (discussed previously, Fig. 2), which show only one <sup>t</sup>Bu resonance as a result of rapid inversion of the SnPh<sub>2</sub> units on the NMR time-scale.

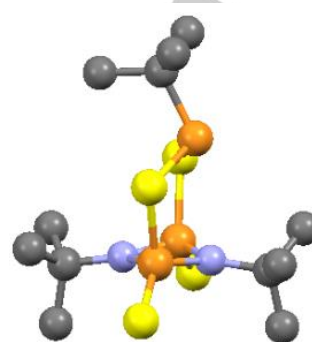


**Fig. 5** Molecular structures of [(**6a**)P<sup>tBu</sup>]. H-atoms have been omitted for clarity. No metric parameters are shown due to the extensive disordering of the structure. Colour code, S (yellow), P (orange), N (violet).

Reaction of the Se-dianion **6b** with I<sub>2</sub> (2 equivalents) or SnCl<sub>4</sub> (1 equivalent) results in oxidation, to give [(S=P(μ-N<sup>t</sup>Bu))<sub>2</sub>(μ-Se-Se-Se-Se)] (**7**) (in 60% yield in the case of I<sub>2</sub>). While the exact mechanism of these reactions is not understood, the same type of reactivity has been reported by Woollins *et al* for the oxidation of the related dianion [BuN=(Se)P(μ-N<sup>t</sup>Bu)]<sub>2</sub><sup>2-</sup> (**5**) with iodine to give [((BuN=)P(μ-N<sup>t</sup>Bu))<sub>2</sub>(μ-Se-Se-Se-Se)], having a similar structure to **7** and containing a Se<sub>4</sub> unit.<sup>[6]</sup> The room-temperature <sup>77</sup>Se NMR spectrum of **7** in C<sub>6</sub>D<sub>6</sub> confirms the presence of two selenium environments, showing a pseudo-triplet resonance centred at  $\delta = 594$  ppm (<sup>2</sup>J<sub>Se-P</sub> = 13 Hz) for the two central Se atoms of the Se<sub>4</sub> unit and a pseudo doublet of doublet resonance centred at  $\delta = 551$  ppm (<sup>1</sup>J<sub>Se-P</sub> = 517.6 Hz, <sup>3</sup>J<sub>Se-P</sub> = 5.5 Hz) for the terminal Se atoms. These NMR characteristics are similar to those reported previously for [((BuN=)P(μ-N<sup>t</sup>Bu))<sub>2</sub>(μ-Se-Se-Se-Se)].<sup>[6]</sup> Confirmation of this arrangement comes from the solid-state structure (Fig. 6).

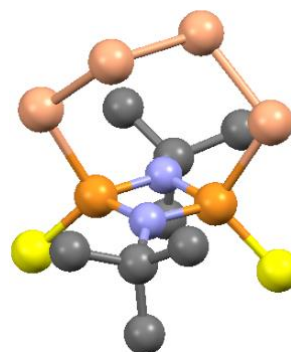


**Fig. 6** Molecular structures of [(S=P(μ-N<sup>t</sup>Bu))<sub>2</sub>(μ-Se-Se-Se-Se)] (**7**). H-atoms and disorder within the Se<sub>4</sub> unit (i.e., a 50 : 50 conformational disordering of the two central Se atoms) have been omitted for clarity. Selected bond lengths (Å) and angles (°): P-S 1.9231(13), P-Se 2.2313(10), Se-Se range 2.267(7)-2.3544(8), P-N range 1.680(3)-1.686(3), P-Se-Se range 101.58(17)-103.63(3), Se-Se-Se range 103.39(3)-104.4(3), S-P-Se 105.62(5), P-N-P 95.48(16), N-P-N 84.44(16). Colour code, S (yellow), P (orange), N (violet), Se (pink).

Studies of the coordination chemistry of the S- and Se-dianions **6a** and **6b** with transition metals have so far involved a limited number of reactions. All reactions involving transition metal salts (like ZnCl<sub>2</sub> and CoCl<sub>2</sub>) not containing supporting

## FULL PAPER

ligands resulted in the formation of insoluble precipitates (most probably polymeric complexes of **6a** and **6b**). The 2 : 1 stoichiometric reaction of the sodium salt of the S-dianion  $[\text{Na}_2(\mathbf{6a})\cdot 0.5\text{thf}]$  with  $\text{Ph}_3\text{PAuCl}$  in thf gives the thf solvate  $[(\text{Ph}_3\text{PAu})_2(\mathbf{6a})]\cdot 2\text{thf}$  (in 15% crystalline yield) (see Supporting Information). In the solid-state structure (Fig. 7) the  $\text{Ph}_3\text{Au}$  units are orientated towards the faces of the  $\text{P}_2\text{N}_2$  of the dianion ligand, i.e., towards the uncoordinated P=S sulfur centers. This unusual arrangement could result from weak intramolecular  $\text{Au}\cdots\text{S}$  interactions, consistent with the deformation of the S-Au-P angle  $[168.79(3)^\circ]$  towards contact with the S-atoms. However, the associated  $\text{Au}\cdots\text{S}$  distances of ca. 3.70 Å are longer than the sum of van der Waals' radii of Au and S (3.50 Å).<sup>[9]</sup> The  $^{31}\text{P}$  NMR spectrum of  $[(\text{Ph}_3\text{Au})_2(\mathbf{6a})]$  at room temperature shows a broad singlet at  $\delta = 32.0$  ppm corresponding to the  $\text{Ph}_3\text{P}$  ligands and a sharp singlet at  $\delta = 78.2$  ppm for the P(V) centers of the  $\text{P}_2\text{N}_2$  ring unit of **6a**. Attempted reaction of the sodium salt of the Se-dianion **6b** with  $\text{Ph}_3\text{PAuCl}$  led only to the formation of colloidal gold.

Room-temperature reaction of the sodium salt of **6b**  $[\text{Na}_2(\mathbf{6b})\cdot 0.5\text{thf}]$  with  $[\text{dppeNiCl}_2]$  in thf gives a red precipitate of the Ni<sup>II</sup> complex  $[(\text{dppeNi})(\mathbf{6b})]$  after 10 minutes (see Supporting Information). Crystals of the solvate  $[(\text{dppeNi})(\mathbf{6b})]\cdot 2\text{CH}_2\text{Cl}_2$  were grown by layering saturated solution of the complex in  $\text{CH}_2\text{Cl}_2$  with *n*-hexane at room-temperature. The solid-state structure reveals the side-on S,Se-coordination of a (dppe)Ni fragment to **6b**, analogous to the side-on N,S-mode found occasionally for  $[\text{BuNH}=(\text{E})\text{P}(\mu\text{-N}^i\text{Bu})_2]^{2-}$  (**5**).<sup>[6]</sup> Fig. 8 shows the idealised structure of molecules of  $[(\text{dppeNi})(\mathbf{6b})]$ . Unfortunately, the 50 : 50 site disordering of the Se and S atoms of the anion **6b** precludes any meaningful discussion of the Ni-ligand bond lengths. However, the structural arrangement is entirely consistent with the room-temperature  $^{31}\text{P}\{^1\text{H}\}$  NMR spectrum in  $\text{CD}_3\text{CN}$ , with the two P atoms of the  $\text{P}_2\text{N}_2$  unit of the dianion **6b** being observed as distinct resonances at  $\delta = 39.7$  and 65.2 ppm. Presumably the Ni center prefers side-on coordination in molecules of  $[(\text{dppeNi})(\mathbf{6b})]$  due to the smaller bite angle of the S,Se-donor site which is closer to the ideal  $90^\circ$  for a square planar environment. Nonetheless, the apparent steric congestion between the <sup>t</sup>Bu of the  $\text{P}_2\text{N}_2$  ring unit and the Ph groups of the dppe ligand results in considerable deviation from an ideal square planar geometry in  $[(\text{dppeNi})(\mathbf{6b})]$ , with the inter-ligand dihedral angle being  $16.2^\circ$  (i.e., the angle between the P-Ni-P and S-Ni-Se planes).

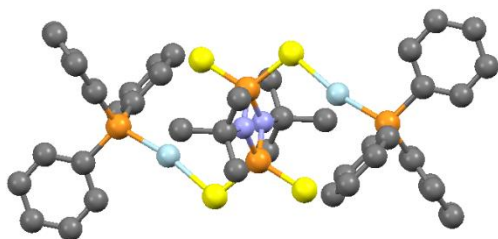


**Fig. 7** Molecular structure of  $[(\text{Ph}_3\text{PAu})_2(\mathbf{6a})]$  in the solvate  $[(\text{Ph}_3\text{PAu})_2(\mathbf{6a})]\cdot 2\text{thf}$ . H-atoms and lattice thf-molecules have been omitted for clarity. Selected bond lengths (Å) and angles ( $^\circ$ ): S-Au 2.3159(9), P-Au 2.2639(10), P-S(Au) 2.0356(16), P=S 1.9430(13), P-N range 1.685(3)–1.692(3), P-Au-S 168.79(3), P-S-Au 104.48(4), P-N-P range 96.21(15), N-P-N 83.79(15). Colour code, S (yellow), P (orange), N (blue), Se (pink), Au (light blue).

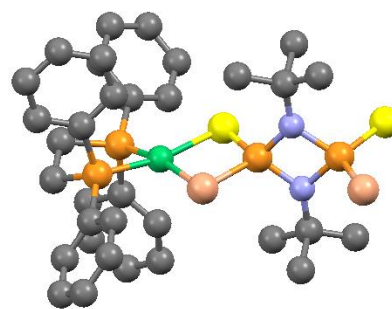


**Fig. 8** Molecular structure of  $[(\text{dppeNi})(\mathbf{6b})]$  in the solvate  $[(\text{dppeNi})(\mathbf{6b})]\cdot 2\text{CH}_2\text{Cl}_2$ . H-atoms and the site 50 : 50 site disorder of the Se and S atoms have been omitted for clarity. Selected bond lengths (Å) and angles ( $^\circ$ ): (dppe)P-Ni 2.1777(7)–2.1778(7), S/Se-Ni 2.3051(5), P-S/Se(Ni) 2.0592(7), P-S/Se 2.1295(7), P-N range 1.652(2)–1.732(3), P-N-P 96.25(13), N-P-N range 81.32(16)–86.17(18). Colour code, S (yellow), P (orange), N (blue), Se (pink), Ni (green).

## Conclusions

We have shown that the oxidation of the P(III) dianion  $[\text{S-P}(\mu\text{-N}^i\text{Bu})_2]^{2-}$  (**1**) gives relatively stable P(V) dianions  $[(\text{S})(\text{E})\text{P}(\mu\text{-N}^i\text{Bu})_2]^{2-}$  (**6**) (for E = S, Se). The latter are sterically un-encumbered relatives of the dianions  $[(\text{E})(\text{RN}=\text{P}(\mu\text{-N}^i\text{Bu})_2]^{2-}$  (**5**), which have previously been investigated by Woollins and Chivers. The coordination chemistry and reactivity of the S,S- and S,Se dianions of **6** are similar to that of **5** but with a more extensive range of coordination modes being made possible by the presence of two 'open' faces in the anion units. Thus, we observe the full array of 'face-on' S,S-, Se,Se- and 'side-on' Se,S-modes in the mixed chalcogen dianion **6b**.

## Acknowledgements

We thank the EU (ERC Advanced Grant for DSW, Erasmus grant for AJP), Cambridge Australia Scholarships (FJR) and the Cambridge Trust (AJP, FJR) and the PPF (AJP) for funding and the Spanish MINECO-AEI and the European Union (ESF) for a Ramon y Cajal contract (RG-R, RYC-2015–19035).

**Keywords:** phosph(III/V)azanes • ambidentate • ligands • main group • transition metal

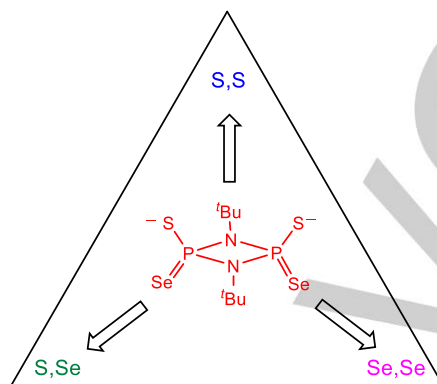
- [1] T. Roth, H. Wadepohl, D. S. Wright, L. H. Gade, *Chem Eur. J.* **2013**, *19*, 13823.
- [2] a) K. V. Axenov, V. V. Kotov, M. Klinga, M. Leskelä, T. Repo, *Eur. J. Inorg. Chem.* **2004**, 695; b) K. V. Axenov, M. Klinga, M. Leskelä, V. Kotov, T. Repo, *Eur. J. Inorg. Chem.* **2004**, 4702; c) K. V. Axenov, M. Leskelä, T. Repo, *J. Catal.* **2006**, 238, 196; d) K. V. Axenov, I. Kilpeläinen, M. Klinga, M. Leskelä, T. Repo, *Organometallics* **2006**, *25*, 463; e) K. V. Axenov, M. Klinga, O. Lehtonen, H. T. Koskela, M. Leskelä, T. Repo, *Organometallics* **2007**, *26*, 1444; f) D. F. Moser, L. Grocholl, L. Stahl, R. J. Staples, *Dalton Trans.* **2003**, 1402; R. Rama Suresh, K. C. Kumara Swamy, *Tet. Let.* **2009**, *50*, 6004.
- [3] a) L. Stahl, *Coord. Chem. Rev.*, **2000**, *210*, 203; b) S. G. González-Calera, D. S. Wright, *Dalton Trans.* **2010**, 39, 5055. M. S. Balakrishna,

- D. J. Eisler, T. Chivers, *Chem. Soc. Rev.* **2007**, 36, 650; M. S. Balakrishna, *Dalton Trans.* **2016**, 45, 12252.
- [4] a) C. G. M. Benson, V. Vasilenko, S. G. Calera, L. H. Gade, D. S. Wright, *Dalton Trans.*, **2015**, 44, 14242; b) C. G. H. Benson, A. Plajer A. D. Bond, S. Singh, L. H. Gade, D. S. Wright, *Chem. Commun.*, **2016**, 52, 9683.
- [5] a) G. G. Briand, T. Chivers, M. Parvez, *Angew. Chem. Int. Ed.* **2002**, 41, 3468; b) T. Chivers, M. Krahn, M. Parvez, G. Schatte, *Inorg. Chem.* **2001**, 40, 2547; (c) see also O. J. Scherer, G. Schnabl, *Angew. Chem. Int. Ed.* **1977**, 16, 486.
- [6] For example, a) T. Chivers, C. Fedorchuk, M. Krahn, M. Parvez, G. Schatte, *Inorg. Chem.* **2001**, 40, 1936; b) A. Nordheider, T. Chivers, R. Thirumoorthi, K. S. A. Arachchige, A. M. Z. Slawin, J. D. Woollins, I. Vargas-Baca, *Dalton Trans.* **2013**, 42, 3291; c) A. Nordheider, T. Chivers, O. Schön, K. Karaghiosoff, K. S. Athukorala Arachchige, A. M. Z. Slawin, J. D. Woollins, *Chem. Eur. J.*, **2014**, 20, 704; d) N. Nordheider, K. Hüll, J. K. D. Prentis, K. S. Athukorala Arachchige, A. M. Z. Slawin, J. D. Woollins, T. Chivers, *Inorg. Chem.* **2015**, 54, 3043; e) N. Nordheider, K. Hüll, K. S. Athukorala Arachchige, A. M. Z. Slawin, J. D. Woollins, R. Thirumoorthi, T. Chivers, *Dalton Trans.* **2015**, 44, 5338; f) A. Nordheider, K. S. A. Arachchige, A. M. Z. Slawin, J. D. Woollins, T. Chivers, *Dalton Trans.* **2015**, 44, 8781.
- [7] Search of the Cambridge Crystallographic Data Base, October 2017.
- [8] A. Nordheider, T. Chivers, R. Thirumoorthi, I. Vargas-Baca, J. D. Woollins, *Chem. Commun.* **2012**, 48, 6346.
- [9] *Inorganic Chemistry: Principles of Structure and Reactivity*, J. Huweey, E. A. Keiter, R. L. Keiter, Harper Collins, 4<sup>th</sup> Ed., **1993**, pp. 290.

## Entry for the Table of Contents

## FULL PAPER

**Three in one:** the new  $P^V$  dianions  $[(S)(E)P(\mu-N^tBu)]_2^{2-}$  ( $E = S, Se, Te$ ) are obtained by reactions of S, Se or Te with the  $P^{III}$  dianion  $[(S)P(\mu-N^tBu)]_2^{2-}$ . The S and Se dianions can readily be transferred intact to main group and transition metal centers, giving a range of new cages and coordination compounds in which the new dianions can exhibit facial S,S- or Se,Se-bonding or side-on S, Se bonding.



A. Plajer, R. Garcia-Rodriguez, F. J. Rizzuto, D. S. Wright.\*

Page No. – Page No.

**Flexible Bonding of the Phosph(V)azane Dianions  $[S(E)P(\mu-N^tBu)]_2^{2-}$**